Semi-classical open string corrections and symmetric Wilson loops

Satoshi YAMAGUCHI

Institut des Hautes Études Scientifiques
35, route de Chartres
91440 – Bures-sur-Yvette (France)

Janvier 2007

IHES/P/07/03

hep-th/yymmnnn
UT-06-22

Correlator of Fundamental and Anti-symmetric Wilson loops in AdS/CFT Correspondence

Ta-Sheng Tai[a*] and Satoshi Yamaguchi[b†]

[a] *Department of Physics, Faculty of Science, University of Tokyo*
Hongo, Bunkyo-ku, Tokyo 113-0033, JAPAN

[b] *IHES, Le Bois-Marie, 35, Route de Chartres F-91440 Bures-sur-Yvette, FRANCE*

Abstract

We study the two circular Wilson loop correlator in which one is of anti-symmetric representation, while the other is of fundamental representation in 4-dimensional $\mathcal{N} = 4$ super Yang-Mills theory. This correlator has a good AdS dual, which is a system of a D5-brane and a fundamental string. We calculated the on-shell action of the string, and clarified the Gross-Ooguri transition in this correlator. Some limiting cases are also examined.

*E-mail:tasheng@hep-th.phys.s.u-tokyo.ac.jp
†E-mail:yamaguch@ihes.fr

Contents

1 Introduction and summary

The Wilson loop is one of the most interesting quantities which appeared in the AdS/CFT correspondence [1]. In the computation of the expectation value of the Wilson loop, the stringy effect (not just the supergravity) is essential. Actually, it is calculated on the AdS side as the on-shell action of a classical macroscopic string[2, 3] in the limit of large N and large 't Hooft coupling $\lambda = 4\pi g_s N = g_{YM}^2 N$.

Recently, certain D-brane pictures of Wilson loops have drawn wide attention because they are powerful in evaluating the Wilson loop of higher rank representation. The D3-brane with electric flux, which has already been investigated in [2], is found to describe Wilson loops of symmetric representations (or multiply wound Wilson loops) by Drukker and Fiol [4]. On the other hand, the Wilson loop of anti-symmetric representation is found to be described by a D5-brane with electric flux[5, 6, 7]. In both cases, the results show successful agreement with the gauge theory side calculations [8, 9]. Other further investigations along this line can be found in [10, 11, 12, 13, 14, 15].

One of the interesting phenomena in the AdS picture of Wilson loops is the phase transition, which occurs in the two Wilson loop correlator. This is first anticipated by

Gross and Ooguri [16], and further explored in [17, 18, 19, 20, 21, 22]. If the two loops are close enough, the classical string of annulus topology leads to the smallest action, which dominates the connected correlator. By contrast, when the two loops get far enough, two disk solution with massless propagating modes dominates the connected correlator. Between them, there exists a critical point.

In this paper, we study two concentric circular Wilson loop correlator of different representations, i.e. one is fundamental and the other is anti-symmetric[1]. Because the circular anti-symmetric Wilson loop has a gravity dual as a D5-brane with electric flux, this correlator can thus be recognized as a system of a D5-brane and an F-string. More explicitly, it is realized as a string which propagates between the AdS boundary and the rigid D5-brane. Here "rigid" means the D5-brane is not pulled by the F-string because of small string coupling $g_s \to 0$.

It is shown that there happens a kind of Gross-Ooguri transition at some critical separation, which arises from the competition of two phases of different worldsheet topologies. This can as well be understood as below. Recall we are assuming that the AdS radius is much larger than the string length l_s. The description of an open string pinned on the D5-brane will no longer persist as the separation gets farther, during when the worldsheet becomes a very thin tube of order l_s. That is, higher stringy correction comes in. Rather, it is reasonable to replace the above picture with a long-range supergraviton exchange, as is usually encountered in the string modular transformation.

We also studied a couple of limiting cases. The solution of two fundamental Wilson loop correlator first examined by Zarembo[17] is recovered, meanwhile the Coulomb-like behavior is found when the separation is much smaller than the circle radii. As a future work, the Yang-Mills side analysis like [23, 24] seems to be interesting. Correlators of Wilson loops of other representations by using the D3-brane [4] or supergravity solutions [25, 26] are as well worthy of study. Also, the extension to finite temperature cases is in progress.

The rest of this paper is organized as follows. In sec.2, the detailed setup is given. In sec.3, the AdS side calculation is performed through a series of elliptic integrals. Finally, in sec.4, we plotted the phase diagram, which visualizes clearly the Gross-Ooguri transition. Comments on these solutions are also provided, where known results appear as limiting cases. Some definitions and algebra involving elliptic integrals are added in the appendix A. The explicit forms of the Coulomb coefficients are shown in appendix B.

[1] Anti-symmetric–anti-symmetric correlator has been studied in [22].

2 Setup

In $\mathcal{N}=4$ Super Yang-Mills theory, the Wilson loop is defined as

$$W_{\mathsf{R}}(C) := \operatorname*{Tr}_{\mathsf{R}}\Big[P\exp\oint_C d\tau(iA_\mu\dot{x}^\mu + \Phi_I n^I(\tau)|\dot{x}|)\Big], \tag{2.1}$$

where A_μ is the gauge field, Φ_I's are six scalar fields, C is a closed trajectory in 4-dimensional spacetime parameterized by τ, n_I is a 6-dimensional unit vector, and R is a representation of SU(N). In this paper, we consider the following type of correlation function

$$\langle W_{A_k}(C_1)W_{\Box}(C_2)\rangle\,. \tag{2.2}$$

We take the trajectories C_1 and C_2 as two circles. Both of them are embedded in a 3-dimensional hyperplane of 4-dimensional space. They are parallel and the centers of them are on the axis which is orthogonal to the circles. If we introduce the Cartesian coordinate x_μ, C_1 is expressed via τ as

$$x_\mu = (0, R_1\cos\tau, R_1\sin\tau, 0), \qquad n^I = (1,0,0,0,0,0), \tag{2.3}$$

while C_2 is

$$x_\mu = (L, R_2\cos\tau, -R_2\sin\tau, 0), \qquad n^I = (\cos\Theta, \sin\Theta, 0,0,0,0), \qquad (0<L,\ 0\le\Theta\le\pi). \tag{2.4}$$

So parameters of this configuration are R_1, R_2, L, Θ.

The correlator (2.2) factorizes in the leading term of the $1/N$ expansion. But this term does not depend on parameters L, R_1, R_2, Θ. In order to see their dependence, the subleading terms become relevant. In other words, what we have to consider is the "connected correlator"

$$\langle W_{A_k}(C_1)W_{\Box}(C_2)\rangle_{conn} = \langle W_{A_k}(C_1)W_{\Box}(C_2)\rangle - \langle W_{A_k}(C_1)\rangle\langle W_{\Box}(C_2)\rangle\,. \tag{2.5}$$

As we will see later, it is convenient to define the function $V_k(R_1,R_2,L,\Theta)$ as

$$V_k(R_1,R_2,L,\Theta) := \frac{\langle W_{A_k}(C_1)W_{\Box}(C_2)\rangle - \langle W_{A_k}(C_1)\rangle\langle W_{\Box}(C_2)\rangle}{\langle W_{A_k}(C_1)\rangle}. \tag{2.6}$$

On the AdS side, this correlation function is described by a system of a D5-brane and a fundamental string subject to certain boundary conditions. The D5-brane is rigid because it is much heavier than the fundamental string. By contrast, the string is flexible, so various kinds of contributions should be considered.

There are two possible leading contributions to V_k. One is a disk bounded by C_2 with massless propagating modes connecting the F-string and the D5-brane (see figure 1). The other is an annulus whose boundaries are attached to the D5-brane and C_2 (see figure

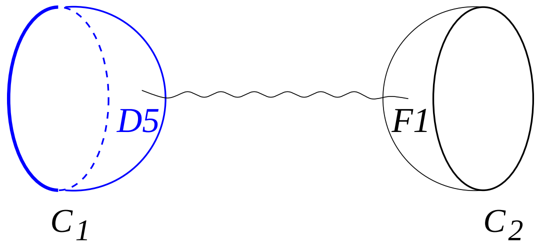

Figure 1: The schematical picture of the disk solution with massless propagating modes. The disk solution is of order $1/g_s$, the massless propagator is of order g_s^2 and the coupling to the D5-brane is of order $1/g_s$. Totally, the contribution is of order g_s^0, which is the same order as the annulus contribution.

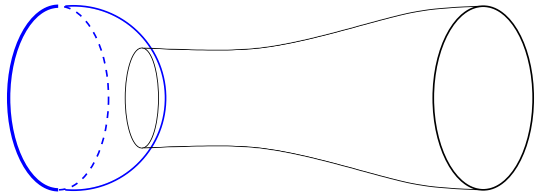

Figure 2: The schematical picture of the annulus. Since the D5-brane is much heavier than the fundamental string, the D5-brane is not deformed. The contribution from this annulus solution is as well of order g_s^0.

2). These two contributions are of the same order $\simeq \mathcal{O}(N^0)$ in $1/N$ expansion. Their magnitudes are estimated by the on-shell action of the annulus and the disk[2], respectively, in large λ limit. In summary, in large λ limit, V_k is approximated as

$$V_k(R_1, R_2, L, \Theta) = \exp(-S_{min}), \tag{2.7}$$

where S_{min} is the global minimum of the string action. The classical on-shell action of the disk, which corresponds to a single circular Wilson loop, has been calculated in [27]. The result is

$$S_{disk,min} = -\sqrt{\lambda}. \tag{2.8}$$

The question now is the competition of (2.8) and that of the annulus. We will investigate the classical annulus solution and compare it with (2.8) in this paper.

Before doing this, we can make some observation upon using the conformal symmetry. There are certain constraints on the correlation function. For example, we have a relation from the dilatation

$$V_k(R_1, R_2, L, \Theta) = V_k(aR_1, aR_2, aL, \Theta), \tag{2.9}$$

where a is a real positive parameter of the dilatation. We can also use the special conformal transformation with a vector parameter b^μ

$$x'^\mu = \frac{x^\mu - b^\mu |x|^2}{1 - 2b^\mu x_\mu + |b|^2 |x|^2}. \tag{2.10}$$

This special conformal transformation (2.10) along x_1, i.e. $b^\mu = (h, 0, 0, 0)$ makes

$$\begin{aligned} &V_k(R_1, R_2, L, \Theta) = V_k(R_1', R_2', L', \Theta), \\ &R_1' = \frac{R_1}{1 + h^2 R_1^2}, \qquad R_2' = \frac{R_2}{1 - 2hL + h^2(L^2 + R_2^2)}, \\ &L' = \frac{L - h(L^2 + R_2^2)}{1 - 2hL + h^2(L^2 + R_2^2)} + \frac{hR_1^2}{1 + h^2 R_1^2}. \end{aligned} \tag{2.11}$$

Therefore, V_k is a function of the invariant combination η as[3]

$$V_k(R_1, R_2, L, \Theta) = \widetilde{V}_k(\eta, \Theta), \qquad \eta = \frac{R_1^2 + R_2^2 + L^2}{2R_1 R_2}. \tag{2.12}$$

On the AdS side, this simple dependence on (η, Θ) is not quite trivial. This is due to the introduction of the cutoff, which makes the conformal symmetry not manifest. However, we will find that the constraint (2.12) is actually satisfied.

[2]The massless propagator contributes a factor of order $\mathcal{O}(\lambda^n)$ to the amplitude. While is compared to $\exp(-\sqrt{\lambda})$, it is thus negligible in large λ limit.

[3]This η plays the same role as the "cross ratio."

3 Classical solution of the annulus

In this section, we will investigate the annulus solution. We use similar techniques employed by [17, 18, 19]. We write down the solution and the corresponding on-shell action. One can see the “phase structure” from the result.

3.1 Ansatz and equations of motion

In this paper, we use the following notation for $AdS_5 \times S^5$ with radius $\sqrt{\alpha'}\lambda^{1/4}$

$$ds^2 = \frac{\alpha'\sqrt{\lambda}}{y^2}(dy^2 + dr^2 + r^2 d\varphi^2 + dt^2 + dx^2) + \alpha'\sqrt{\lambda}(d\theta^2 + \sin^2\theta d\Omega_4^2). \tag{3.1}$$

The boundary of AdS_5 is at $y = 0$. The coordinate (r, φ, t, x) at the boundary is related to the Cartesian coordinate x_μ introduced in the previous section as

$$x_1 = x, \qquad x_2 = r\cos\varphi, \qquad x_3 = r\sin\varphi, \qquad x_4 = t. \tag{3.2}$$

The string dual of $W_{A_k}(C_1)$ is a D5-brane [6, 7]. Its explicit form[28, 29] is expressed as

$$r^2 + y^2 = R_1^2, \qquad \theta = \theta_k, \tag{3.3}$$

where R_1 is the radius of C_1, and θ_k is related to k as

$$\frac{k}{N} = \frac{1}{\pi}\left(\theta_k - \frac{1}{2}\sin 2\theta_k\right). \tag{3.4}$$

The gauge field excitation on the D5-brane worldvolume has the field strength

$$\mathcal{F}_{y\varphi} = -i\cos\theta_k \frac{\alpha'\sqrt{\lambda}R_1}{y^2}, \qquad \mathcal{F} := 2\pi\alpha' dA. \tag{3.5}$$

The worldsheet stretching between this D5-brane and C_2 is symmetric under the rotation $\varphi \to \varphi + \alpha$, α: real constant parameter. Hence, we can assign this symmetry to our solution. The reparameterization degrees of freedom enable one to set the worldsheet coordinates as (σ, φ), where φ is the same as the spacetime φ. The ansatz used is written as

$$y = y(\sigma), \qquad r = r(\sigma), \qquad x = x(\sigma), \qquad \theta = \theta(\sigma). \tag{3.6}$$

In this ansatz, we include σ dependence of θ because the two boundaries are separated in S^5 in general, i.e. the D5-brane is wrapped on an S^4 at $\theta = \theta_k$, while C_2 sits on a point $\theta = \Theta$ in S^5.

The bulk part comes from the Nambu-Goto action

$$S_{bulk} = \frac{1}{2\pi\alpha'}\int d\sigma d\varphi \sqrt{\det G}, \tag{3.7}$$

where G is the induced metric. Plugging (3.6) and integrating out φ, we obtain

$$S_{bulk} = \int d\sigma \mathcal{L}, \qquad \mathcal{L} = \sqrt{\lambda}\frac{r}{y^2}\sqrt{x'^2 + r'^2 + y'^2 + y^2\theta'^2}, \tag{3.8}$$

where prime $'$ denotes the σ derivative.

At both boundaries, we need to include proper boundary terms. Let $\sigma = \sigma_1$ be the boundary on the D5-brane, whereas $\sigma = \sigma_2$ be the boundary at C_2 with $\sigma_1 < \sigma_2$. At $\sigma = \sigma_1$, the boundary is constrained on the rigid D5-brane in (3.3), and should satisfy at least the following conditions

$$r^2 + y^2 = R_1^2, \qquad x = 0, \qquad \theta = \theta_k. \tag{3.9}$$

These are not all the conditions however. Due to the gauge field excitation in (3.5), we should add

$$S_{bdy,1} = i\oint_{\sigma=\sigma_1} d\varphi\ A_\varphi\ + (\text{constant}) = \sqrt{\lambda}\cos\theta_k\left(1 - \frac{R_1}{y}\right), \quad A_\varphi = \frac{1}{2\pi\alpha'} i\cos\theta_k \frac{\alpha'\sqrt{\lambda}R_1}{y}. \tag{3.10}$$

The (constant) ensures that $S_{bdy,1} = 0$ when $y = R_1$, where the circle of φ shrinks to a point. The boundary condition is derived from the variational principle. The variation of the bulk action has boundary terms at $\sigma = \sigma_1$ as

$$\delta S_{bulk}|_{bdy,1} = -\, p_r\delta r - p_y\delta y - p_x\delta x - p_\theta\delta\theta. \tag{3.11}$$

The momenta p are written as

$$p_r = \sqrt{\lambda}\frac{r}{y^2}\frac{r'}{\sqrt{x'^2 + r'^2 + y'^2 + y^2\theta'^2}}, \tag{3.12}$$

$$p_y = \sqrt{\lambda}\frac{r}{y^2}\frac{y'}{\sqrt{x'^2 + r'^2 + y'^2 + y^2\theta'^2}}, \tag{3.13}$$

$$p_x = \sqrt{\lambda}\frac{r}{y^2}\frac{x'}{\sqrt{x'^2 + r'^2 + y'^2 + y^2\theta'^2}}, \tag{3.14}$$

$$p_\theta = \sqrt{\lambda}\frac{r\theta'}{\sqrt{x'^2 + r'^2 + y'^2 + y^2\theta'^2}}. \tag{3.15}$$

Due to $r^2 + y^2 = R_1$, it is convenient to rewrite (3.11) as

$$\delta S_{bulk}|_{bdy,1} = -\frac{1}{2}\left(\frac{p_r}{r} + \frac{p_y}{y}\right)(r\delta r + y\delta y) - \frac{1}{2}\left(\frac{p_r}{r} - \frac{p_y}{y}\right)(r\delta r - y\delta y) - p_x\delta x - p_\theta\delta\theta. \tag{3.16}$$

On the other hand, the variation of $S_{bdy,1}$ is written as (using the condition $r\delta r + y\delta y = 0$)

$$\delta S_{bdy,1} = -\frac{1}{2}\sqrt{\lambda}\cos\theta_k\frac{R_1}{y^3}(r\delta r - y\delta y). \tag{3.17}$$

We obtain totally

$$\delta S_{bulk}|_{bdy,1} + \delta S_{bdy,1} = -\frac{1}{2}\left(\frac{p_r}{r} + \frac{p_y}{y}\right)(r\delta r + y\delta y) - \frac{1}{2}\left(\frac{p_r}{r} - \frac{p_y}{y} + \sqrt{\lambda}\cos\theta_k \frac{R_1}{y^3}\right)(r\delta r - y\delta y)$$

$$- p_x\delta x - p_\theta\delta\theta. \tag{3.18}$$

The first, third and fourth term vanish because of (3.9). From the second term, it can be seen that the additional boundary condition at $\sigma = \sigma_1$ is

$$\frac{p_r}{r} - \frac{p_y}{y} + \sqrt{\lambda}\cos\theta_k \frac{R_1}{y^3} = 0. \tag{3.19}$$

Next, let us turn to the other boundary at $\sigma = \sigma_2$. Naively, the area of the minimal surface is infinite. It is necessary to introduce a cutoff at $y = \epsilon$ in order to regularize the action. We follow [30] and perform the Legendre transformation. This gives a boundary term

$$S_{bdy,2} = -p_y y - p_\theta(\theta - \Theta), \qquad \text{at } \sigma = \sigma_2. \tag{3.20}$$

Now we solve the equations of motion subject to the above boundary conditions. Each equation of motion of r, y, x, θ, respectively, derived from (3.8) can be listed as

$$\frac{1}{y^2}\sqrt{x'^2 + r'^2 + y'^2 + y^2\theta'^2} - \partial_\sigma\left(\frac{r}{y^2}\frac{r'}{\sqrt{x'^2 + r'^2 + y'^2 + y^2\theta'^2}}\right) = 0, \tag{3.21}$$

$$-2\frac{r}{y^3}\sqrt{x'^2 + r'^2 + y'^2 + y^2\theta'^2} + \frac{r}{y}\frac{\theta'^2}{\sqrt{x'^2 + r'^2 + y'^2 + y^2\theta'^2}} - \partial_\sigma\left(\frac{r}{y^2}\frac{y'}{\sqrt{x'^2 + r'^2 + y'^2 + y^2\theta'^2}}\right) = 0, \tag{3.22}$$

$$\partial_\sigma\left(\frac{r}{y^2}\frac{x'}{\sqrt{x'^2 + r'^2 + y'^2 + y^2\theta'^2}}\right) = 0, \tag{3.23}$$

$$\partial_\sigma\left(\frac{r\theta'}{\sqrt{x'^2 + r'^2 + y'^2 + y^2\theta'^2}}\right) = 0. \tag{3.24}$$

Following [17, 18], we integrate (3.23), (3.24) and fix the reparameterization of σ as $x = \sigma$ to obtain

$$\frac{r}{y^2}\frac{1}{\sqrt{1 + r'^2 + y'^2 + y^2\theta'^2}} = \ell, \tag{3.25}$$

$$\frac{r\theta'}{\sqrt{1 + r'^2 + y'^2 + y^2\theta'^2}} = m, \tag{3.26}$$

where ℓ and m are integration constants. We can assume $\ell > 0$ without loss of generality. Plugging these into (3.21) and (3.22), we obtain

$$\frac{r}{\ell^2 y^4} - r'' = 0, \tag{3.27}$$

$$-\frac{2r^2}{\ell^2 y^5} + \frac{m^2}{\ell^2 y^3} - y'' = 0, \tag{3.28}$$

and they combine to be

$$0 = 1 + r'^2 + y'^2 - \frac{r^2}{\ell^2 y^4} + \frac{m^2}{\ell^2 y^2}. \tag{3.29}$$

Adding (3.27) multiplied by r to (3.28) multiplied by y leads to

$$(r^2 + y^2)'' + 2 = 0. \tag{3.30}$$

This equation is integrated to be

$$r^2 + y^2 + (x + c)^2 = a^2, \tag{3.31}$$

where a and c are integration constants. At $x = 0$ (D5-brane side), $r^2 + y^2 = R_1^2$ leads to

$$a^2 - c^2 = R_1^2, \tag{3.32}$$

while at $x = L$ (AdS boundary,) $r = R_2$ and $y = 0$ lead to

$$a^2 - (L + c)^2 = R_2^2. \tag{3.33}$$

Based on these, a and c can be expressed in terms of R_1, R_2, L as

$$c = \frac{R_1^2 - R_2^2 - L^2}{2L}, \qquad a = \frac{\sqrt{(R_1^2 + R_2^2 + L^2)^2 - 4R_1^2 R_2^2}}{2L}. \tag{3.34}$$

By using the trigonometric parameterization

$$r = \sqrt{a^2 - (x + c)^2}\cos\phi, \qquad y = \sqrt{a^2 - (x + c)^2}\sin\phi, \qquad 0 \le \phi \le \frac{\pi}{2}, \tag{3.35}$$

(3.29) becomes

$$\phi' = \pm\left(\frac{a}{a^2 - (x + c)^2}\right)\frac{\sqrt{\cos^2\phi - m^2\sin^2\phi - \ell^2 a^2 \sin^4\phi}}{\ell a \sin^2\phi}. \tag{3.36}$$

Furthermore, the boundary condition (3.19) can be rewritten as a constraint on $\phi_1 := \phi(0)$ and $\phi'(0)$ as

$$\phi'(0) = \cos\theta_k \frac{\sin\phi_1}{\ell R_1^2 \cos^2\phi_1}, \tag{3.37}$$

where we have used (3.35). Also, (3.37) and (3.36) lead to the expression of ϕ_1 as

$$\sin^2\phi_1 = \frac{-(m^2+\sin^2\theta_k)+\sqrt{(m^2+\sin^2\theta_k)^2+4\ell^2a^2\sin^2\theta_k}}{2\ell^2a^2}. \tag{3.38}$$

Finally, (3.26) can be rewritten as

$$\theta' = \frac{m}{\ell(a^2-(x+c)^2)\sin^2\phi} \tag{3.39}$$

by using (3.25) and (3.35). This and (3.36) together lead to

$$\frac{d\phi}{d\theta} = \frac{\phi'}{\theta'} = \pm\frac{1}{m}\sqrt{\cos^2\phi - m^2\sin^2\phi - \ell^2a^2\sin^4\phi}. \tag{3.40}$$

Now, we have almost done. Note that (3.36) and (3.40) can be easily integrated. The remaining subtlety is to choose the right branch from them. At $x=0$, we find that the sign of $\phi'(0)$ is determined by the sign of $\cos\theta_k$ from (3.37). We will examine two cases: $\theta_k > \pi/2$ and $\theta_k < \pi/2$ in turn. The case of $\theta_k = \pi/2$ is realized as the limit of either case.

3.2 $\theta_k > \pi/2$: monotonically decreasing ϕ

When $\theta_k > \pi/2$, $\phi'(0)$ is negative by virture of (3.37), i.e. around $x=0$, ϕ decreases. Defining what inside the square root in (3.36) as a function of ϕ :

$$\mathcal{H}(\phi) := \cos^2\phi - m^2\sin^2\phi - \ell^2a^2\sin^4\phi, \tag{3.41}$$

we see that $\mathcal{H}(\phi)$ is a monotonically decreasing function on $0 \le \phi \le \pi/2$, and $\mathcal{H}(\phi_1) > 0$ according to (3.38). Hence as ϕ decreases, $\mathcal{H}$ becomes bigger and never reaches the branching point $\mathcal{H} = 0$. Therefore, $\phi(x)$ is a monotonically decreasing function over $0 \le x \le L$. We thus take the minus sign in (3.36), (3.40), and then integrate them to obtain

$$\int_{\phi_1}^{\phi} \frac{\ell a \sin^2\psi d\psi}{\sqrt{\cos^2\psi - m^2\sin^2\psi - \ell^2a^2\sin^4\psi}} = -\frac{1}{2}\log\frac{a+x+c}{a-x-c} + \frac{1}{2}\log\frac{a+c}{a-c}, \tag{3.42}$$

$$\int_{\phi_1}^{\phi} \frac{m d\psi}{\sqrt{\cos^2\psi - m^2\sin^2\psi - \ell^2a^2\sin^4\psi}} = -\theta + \theta_k. \tag{3.43}$$

Note that $\phi(x)$ and $\theta(x)$ can be completely fixed by solving the above equations implemented with the boundary conditions :

$$\phi(L) = 0, \qquad \theta(L) = \Theta, \tag{3.44}$$

which in turn determine m and ℓ. To see this more explicitly, it is convenient to introduce

$$f(m,\ell a)=\int_0^{\phi_1}\frac{\ell a\sin^2\psi d\psi}{\sqrt{\cos^2\psi-m^2\sin^2\psi-\ell^2a^2\sin^4\psi}}, \tag{3.45}$$

$$g(m,\ell a)=\int_0^{\phi_1}\frac{m d\psi}{\sqrt{\cos^2\psi-m^2\sin^2\psi-\ell^2a^2\sin^4\psi}}. \tag{3.46}$$

Rewriting the L.H.S. of (3.42) at $x=L$ via (3.34) into

$$\begin{aligned}-\frac{1}{2}\log\frac{a+L+c}{a-L-c}+\frac{1}{2}\log\frac{a+c}{a-c}&=-\log\frac{R_1^2+R_2^2+L^2+\sqrt{(R_1^2-R_2^2)^2+L^4+2L^2(R_1^2+R_2^2)}}{2R_1R_2}\\&=-\log\left[\eta+\sqrt{\eta^2-1}\right],\end{aligned} \tag{3.47}$$

where η is defined in (2.12), we can re-express (3.44) as

$$\cosh[f(m,\ell a)]=\eta,\qquad g(m,\ell a)=\Theta-\theta_k. \tag{3.48}$$

Namely, m and ℓa are determined in terms of η,Θ if exist. Let us compute the on-shell action. The bulk action (3.8) now takes the form

$$S_{bulk}=\sqrt{\lambda}\int_0^L dx\frac{r}{y^2}\sqrt{1+r'^2+y'^2+y^2\theta'^2}=\sqrt{\lambda}\int_{\frac{\epsilon}{R_2}}^{\phi_1}\frac{d\phi\cot^2\phi}{\sqrt{\cos^2\phi-m^2\sin^2\phi-\ell^2a^2\sin^4\phi}}, \tag{3.49}$$

where we have put a cutoff at $y=\epsilon$. We ignore terms which vanish when $\epsilon\to0$. Also, there are two boundary terms

$$x=0,\qquad S_{bdy,1}=\sqrt{\lambda}\cos\theta_k(1-\csc\phi_1), \tag{3.50}$$

$$x=L,\qquad S_{bdy,2}=-\sqrt{\lambda}\frac{R_2}{\epsilon}, \tag{3.51}$$

from (3.10) and (3.20), respectively. The total on-shell action is $S_{tot}=S_{bulk}+S_{bdy,1}+S_{bdy,2}$.

Here we summarize the result of this subsection. When $\theta_k>\pi/2$, the on-shell action can be written by using the formulas in appendix A.2 as

$$\begin{aligned}\frac{S_{tot}}{\sqrt{\lambda}}=&[(m^2+1)^2+4\ell^2a^2]^{1/4}\Bigg[-\cot\chi(\phi_1)\sqrt{1-\kappa^2\sin^2\chi(\phi_1)}-E(\chi(\phi_1),\kappa)\\&+(1-\kappa^2)F(\chi(\phi_1),\kappa)\Bigg]+\cos\theta_k(1-\csc\phi_1).\end{aligned} \tag{3.52}$$

Note that ϕ_1 is defined in (3.38), whereas $\chi(\phi), \kappa$ and C are defined in (A.17). Here F and E are the elliptic integrals of the first and second kind, respectively. The integration constants $m, \ell a$ are determined by

$$\operatorname{arccosh}\eta = \frac{(m^2+1)+\sqrt{(m^2+1)^2+4\ell^2a^2}}{2\ell a\left[(m^2+1)^2+4\ell^2a^2\right]^{1/4}}\left[\Pi(\chi(\phi_1),C,\kappa)-F(\chi(\phi_1),\kappa)\right], \tag{3.53}$$

$$\Theta-\theta_k = m[(m^2+1)^2+4\ell^2a^2]^{-1/4}F(\chi(\phi_1),\kappa), \tag{3.54}$$

where Π is the elliptic integral of the third kind. We found that this result satisfies the conformal symmetry condition indicated in (2.12).

3.3 $\theta_k < \pi/2$: increasing and decreasing ϕ

When $\theta_k < \pi/2$, $\phi'(0)$ is positive by virtue of (3.37). Note that ϕ keeps increasing from $x=0$ (during when $\mathcal{H}$ in (3.41) decreases) untill the branching point ($\mathcal{H}=0$) is reached at $x=x_0$. This causes a sign change in (3.36) and (3.40) such that ϕ starts to decrease all the way to zero at $x=L$. Consequently, we take the plus branch for $x \le x_0$, and the minus branch for $x \ge x_0$ in (3.36) and (3.40).

It is convenient to define $\phi_0 := \phi(x_0)$, which satisfies $\mathcal{H}(\phi_0)=0$ and can be solved as

$$\sin^2\phi_0 = \frac{-(m^2+1)+\sqrt{(m^2+1)^2+4\ell^2a^2}}{2\ell^2a^2}. \tag{3.55}$$

When $x \le x_0$, integrating (3.36) and (3.40) gives

$$\int_{\phi_1}^{\phi}\frac{\ell a\sin^2\psi d\psi}{\sqrt{\cos^2\psi-m^2\sin^2\psi-\ell^2a^2\sin^4\psi}} = \frac{1}{2}\log\frac{a+x+c}{a-x-c}-\frac{1}{2}\log\frac{a+c}{a-c}, \tag{3.56}$$

$$\int_{\phi_1}^{\phi}\frac{m d\psi}{\sqrt{\cos^2\psi-m^2\sin^2\psi-\ell^2a^2\sin^4\psi}} = \theta-\theta_k. \tag{3.57}$$

On the other hand, when $x \ge x_0$,

$$\left(\int_{\phi_1}^{\phi_0}-\int_{\phi_0}^{\phi}\right)\frac{\ell a\sin^2\psi d\psi}{\sqrt{\cos^2\psi-m^2\sin^2\psi-\ell^2a^2\sin^4\psi}} = \frac{1}{2}\log\frac{a+x+c}{a-x-c}-\frac{1}{2}\log\frac{a+c}{a-c}, \tag{3.58}$$

$$\left(\int_{\phi_1}^{\phi_0}-\int_{\phi_0}^{\phi}\right)\frac{m d\psi}{\sqrt{\cos^2\psi-m^2\sin^2\psi-\ell^2a^2\sin^4\psi}} = \theta-\theta_k. \tag{3.59}$$

We again define

$$\tilde{f}(m,\ell a) = \left(\int_{\phi_1}^{\phi_0}+\int_{0}^{\phi_0}\right)\frac{\ell a\sin^2\psi d\psi}{\sqrt{\cos^2\psi-m^2\sin^2\psi-\ell^2a^2\sin^4\psi}}, \tag{3.60}$$

$$\tilde{g}(m,\ell a) = \left(\int_{\phi_1}^{\phi_0}+\int_{0}^{\phi_0}\right)\frac{m d\psi}{\sqrt{\cos^2\psi-m^2\sin^2\psi-\ell^2a^2\sin^4\psi}} \tag{3.61}$$

as before in order to incorporate the boundary condition (3.44). (3.58), (3.59) and (3.44) lead to

$$\eta = \cosh[\tilde{f}(m, \ell a)], \qquad \tilde{g}(m, \ell a) = \Theta - \theta_k. \tag{3.62}$$

Here, m and ℓa are determined in terms of η, Θ if exist. The on-shell action S_{tot} contains the bulk part

$$S_{bulk} = \sqrt{\lambda}\left(\int_{\phi_1}^{\phi_0} + \int_{\frac{\epsilon}{R_2}}^{\phi_0}\right) \frac{d\phi \cot^2 \phi}{\sqrt{\cos^2 \phi - m^2 \sin^2 \phi - \ell^2 a^2 \sin^4 \phi}} \tag{3.63}$$

as well as boundary terms which are the same as (3.50) and (3.51).

We summarize the result of this subsection. When $\theta_k < \pi/2$, the on-shell action can be written by using the formulas in appendix A.2 as

$$\begin{aligned}\frac{S_{tot}}{\sqrt{\lambda}} =& [(m^2+1)^2 + 4\ell^2 a^2]^{1/4} \Bigg[\cot \chi(\phi_1) \sqrt{1 - \kappa^2 \sin^2 \chi(\phi_1)} \\ & + E(\chi(\phi_1), \kappa) - (1-\kappa^2) F(\chi(\phi_1), \kappa) - 2E(\kappa) + 2(1-\kappa^2) K(\kappa) \Bigg] + \cos \theta_k (1 - \csc \phi_1),\end{aligned} \tag{3.64}$$

where ϕ_1 is defined in (3.38), while $\chi(\phi)$, κ, and C are defined in (A.17). The integration constants $m, \ell a$ are determined by

$$\operatorname{arccosh} \eta = \frac{(m^2+1) + \sqrt{(m^2+1)^2 + 4\ell^2 a^2}}{2\ell a \left[(m^2+1)^2 + 4\ell^2 a^2\right]^{1/4}} \left[2\Pi(C, \kappa) - 2K(\kappa) - \Pi(\chi(\phi_1), C, \kappa) + F(\chi(\phi_1), \kappa)\right], \tag{3.65}$$

$$\Theta - \theta_k = m[(m^2+1)^2 + 4\ell^2 a^2]^{-1/4} [2K(\kappa) - F(\chi(\phi_1), \kappa)]. \tag{3.66}$$

Again, the conformal symmetry condition in (2.12) is satisfied.

4 Comments on the solutions

4.1 Gross-Ooguri phase transition

Let us consider the Gross-Ooguri (GO) phase transition here. We compare (3.52)-(3.54) (or (3.64)-(3.66), when $\theta_k < \pi/2$) and (2.8). We are also interested in how far the annulus solution can stretch along η. For example, when $\theta_k > \pi/2$, the annulus solution exists, if and only if (3.53) and (3.54) can be solved by some $(m, \ell a)$ for a given (η, Θ) pair.

Figures 3, 4 and 5 present the phase diagrams plotted against the η-Θ plane at $\theta_k = \pi/2$, $2\pi/3$ and $\pi/3$, respectively. The black solid line indicates the critical line of the

GO phase transition. The red dashed line stands for the critical line where the annulus solution becomes unstable. One finds that $\Theta = \pi$ is always in the disk phase. This observation has a good explanation. When $\Theta = \pi$, two loops overlap ($\eta = 1$) so that this configuration becomes BPS. Therefore, the annulus solution does not exist.

In addition, the Θ dependence of the phase diagram is interesting. The critical distance marks a maximum at $\Theta = \theta_k$ when θ_k is fixed. This fact is quite reasonable from the AdS point of view. However, it is rather mysterious from the gauge theory side since Θ and θ_k have rather different origins; Θ is the direction of the scalar as in (2.4), while θ_k is determined by the rank of the anti-symmetric representation as in (3.4). To consider this fact from the gauge theory is an interesting future work.

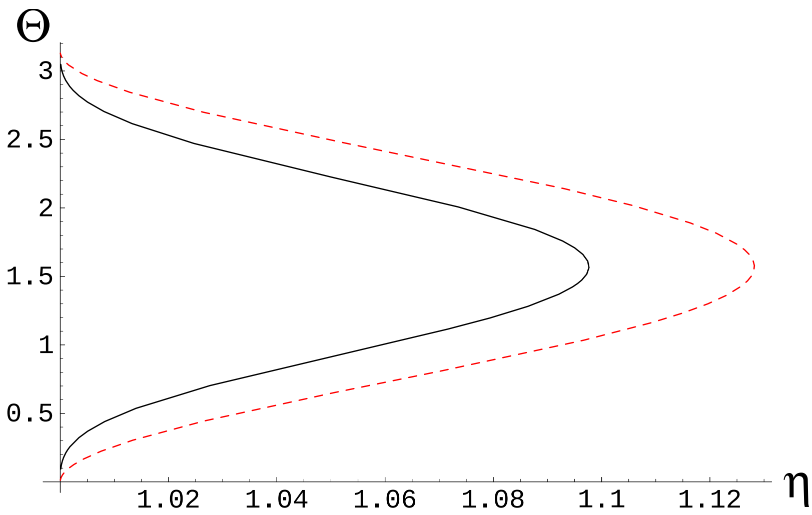

Figure 3: Phase diagram on η-Θ plane with $\theta_k = \pi/2$. The solid black line indicates the critical line of the GO transition. Inside (outside) the solid line, the annulus (disk) solution dominates the connected correlator. The red dashed line represents the critical line where the annulus solution becomes unstable. The annulus solution does not exist outside the red dashed line.

4.2 $k = 1$

It is illuminating to check some limiting aspects of the above solutions. When $k = 1$, the k-th anti-symmetric representation reduces to the fundamental one. So, assuming $k = 1$ and $\Theta = 0$, one may expect (3.64)-(3.66) reproduce the correlator of two fundamental loops. We will see this is actually the case, and it is somewhat non-trivial in the sense that the D5-brane picture of the anti-symmetric loop is valid only when k is large and comparable to N. From (3.4), it is seen that $\lim_{k\to 1} \theta_k \cong \left(\frac{3\pi}{2N}\right)^{1/3} \ll 1$. Since we have fixed $\Theta = 0$ here, the L.H.S. of (3.66) is much smaller than 1. This means that $m \ll 1$ because other factors in the R.H.S. of (3.66) are finite. Due to $\theta_k \ll 1$ and $m \ll 1$, one

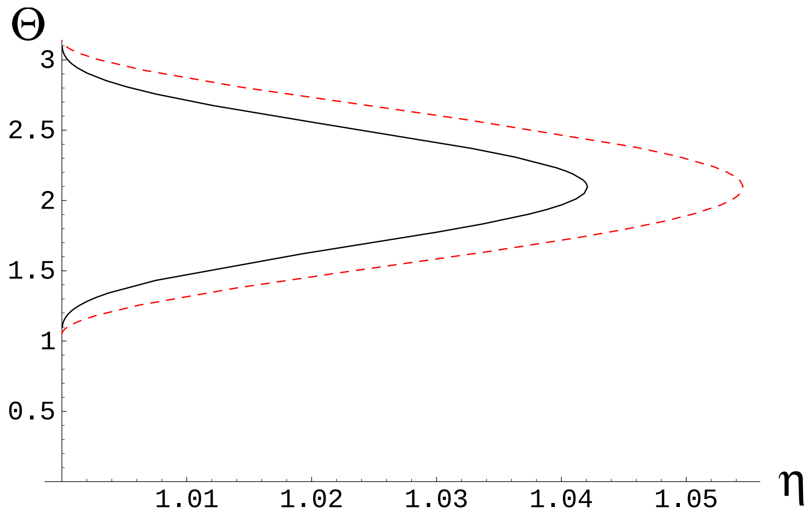

Figure 4: Phase diagram on η-Θ plane with $\theta_k = 2\pi/3$.

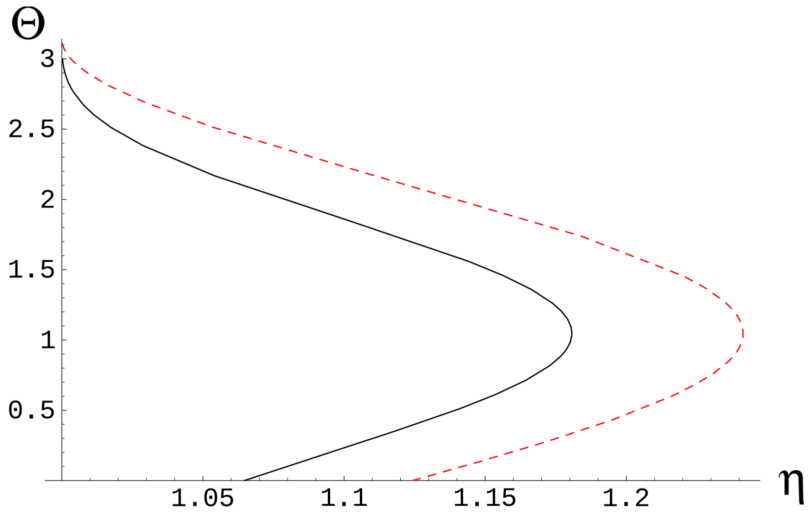

Figure 5: Phase diagram on η-Θ plane with $\theta_k = \pi/3$.

finds $\phi_1 \ll 1$ by using (3.38). This means that the end on the D5-brane is drawn closely to the AdS boundary.

Taking these facts into account, we can express the results (3.64)-(3.66) for $k = 1$ as

$$\operatorname{arccosh}\eta = \frac{1+\sqrt{1+4\ell^2a^2}}{\ell a(1+4\ell^2a^2)^{1/4}}\left[\Pi(C,\kappa) - K(\kappa)\right], \qquad \kappa^2 = \frac{1}{2} + \frac{1}{2\sqrt{1+4\ell^2a^2}}, \tag{4.1}$$

$$S_{tot} = \sqrt{\lambda} + 2\sqrt{\lambda}\left[1+4\ell^2a^2\right]^{1/4}\left[-E(\kappa) + (1-\kappa^2)K(\kappa)\right]. \tag{4.2}$$

Recall that S_{tot} is identified with $-\log V_k$ in (2.7). The first term in S_{tot} is interpreted as the contribution from the denominator in (2.6). The second term and (4.1) are completely the same as the ones in the correlator of two fundamental Wilson loops, see [17, 18, 19].

4.3 Limit to anti-parallel lines

When $R_1 = R_2 \gg L$, the Wilson loop correlator reduces to the anti-parallel lines. In this case, one expects that the correlator exhibits the Coulomb's law as

$$-\log V_k(R_1, R_2, L, \Theta) \cong 2\pi R_2 \frac{M}{L}, \tag{4.3}$$

where M is a constant determined by k and Θ. In terms of ℓ and m, this limit is realized via $\ell a \to \infty$ with $\gamma = \frac{m^2}{2\ell a}$ fixed. The explicit form of the coefficient M is written down in appendix B.

Acknowledgements

We would like to thank Changhyun Ahn, Yosuke Imamura, Feng-Li Lin, Yutaka Matsuo, Nikita Nekrasov, Soo-Jong Rey and Jung-Tay Yee for useful discussions and comments. The work of S.Y. was supported in part by the European Research Training Network contract 005104 "ForcesUniverse."

A Elliptic integrals

A.1 Definitions and some formulas of the standard elliptic integrals

$$F(\varphi, k) := \int_0^{\sin\varphi} dz \frac{1}{\sqrt{(1-z^2)(1-k^2z^2)}}, \tag{A.1}$$

$$E(\varphi, k) := \int_0^{\sin\varphi} dz \sqrt{\frac{1-k^2z^2}{1-z^2}}, \tag{A.2}$$

$$\Pi(\varphi, C, k) := \int_0^{\sin\varphi} dz \frac{1}{(1-Cz^2)\sqrt{(1-z^2)(1-k^2z^2)}}. \tag{A.3}$$

Complete elliptic integrals are

$$K(k) := F(\pi/2, k), \qquad E(k) := E(\pi/2, k), \qquad \Pi(C, k) := \Pi(\pi/2, C, k). \tag{A.4}$$

When $C = k^2$, the third elliptic integral is related to the second one as

$$\Pi(\varphi, k^2, k) = \frac{1}{1-k^2} E(\varphi, k) - \frac{k^2}{1-k^2} \frac{\sin\varphi\cos\varphi}{\sqrt{1-k^2\sin^2\varphi}}. \tag{A.5}$$

Let a, b, c, d be four real constants which satisfies $a < b < c < d$. We assume the real variable u satisfies $b \leq u \leq c$. If two variable u and z are related as

$$z^2 := \frac{(c-a)(u-b)}{(c-b)(u-a)}, \quad \text{or} \quad u = \frac{(c-a)b - (c-b)az^2}{(c-a) - (c-b)z^2}, \tag{A.6}$$

there is a 1-form relation

$$\frac{du}{\sqrt{(u-a)(u-b)(u-c)(u-d)}} = \frac{2}{\sqrt{(c-a)(d-b)}} \frac{dz}{\sqrt{(1-z^2)(1-k^2z^2)}}, \tag{A.7}$$

$$k^2 := \frac{(c-b)(d-a)}{(c-a)(d-b)}. \tag{A.8}$$

We obtain the following formula.

$$\int_b^v \frac{du}{\sqrt{(u-a)(u-b)(u-c)(u-d)}} = \frac{2}{\sqrt{(c-a)(d-b)}} F(\varphi, k), \tag{A.9}$$

$$\sin\varphi := \frac{(c-a)(v-b)}{(c-b)(v-a)}. \tag{A.10}$$

$$\int_b^v du \sqrt{\frac{(u-b)}{(u-a)(u-c)(u-d)}} = \frac{2(b-a)}{\sqrt{(c-a)(d-b)}} \left[\Pi(\varphi, C, k) - F(\varphi, k)\right], \tag{A.11}$$

$$C = \frac{c-b}{c-a}. \tag{A.12}$$

Let δ be a small number.

$$\int_{b+\delta}^v \frac{1}{(u-b)\sqrt{(u-a)(u-b)(u-c)(u-d)}} =$$

$$\frac{2}{\sqrt{(c-a)(d-b)}} \left\{ \sqrt{\frac{c-a}{(c-b)(b-a)}} \frac{1}{\sqrt{\delta}} - \frac{(c-a)}{(c-b)(b-a)} \cot\varphi \sqrt{1-k^2\sin^2\varphi} \right.$$

$$\left. - \frac{(c-a)}{(c-b)(b-a)} E(\varphi, k) + \frac{1}{c-b} F(\varphi, k) \right\} + (\text{terms vanishing when } \delta \to 0). \tag{A.13}$$

In order to derive this formula, the relation

$$\frac{1}{z^2\sqrt{(1-z^2)(1-k^2z^2)}} = \frac{d}{dz}\left[\frac{-1}{z}\sqrt{(1-z^2)(1-k^2z^2)}\right] + \sqrt{\frac{1-k^2z^2}{1-z^2}} + \sqrt{(1-z^2)(1-k^2z^2)} \tag{A.14}$$

is useful.

A.2 Expressions of some integrals in terms of the standard elliptic integrals

$$u = \sin^2\psi, \qquad v = \sin^2\phi, \qquad \beta_\pm = \frac{-(m^2+1) \pm \sqrt{(m^2+1)^2 + 4\ell^2a^2}}{2\ell^2a^2}, \tag{A.15}$$

where $\beta_- < 0 \le v \le \beta_+ < 1$, and

$$\frac{d\psi}{\sqrt{\cos^2\psi - m^2\sin^2\psi - \ell^2a^2\sin^4\psi}} = \frac{du}{2\ell a\sqrt{(u-\beta_-)u(u-\beta_+)(u-1)}}. \tag{A.16}$$

$$\kappa := \sqrt{\frac{\beta_+(1-\beta_-)}{\beta_+-\beta_-}}, \qquad C := \frac{\beta_+}{\beta_+-\beta_-}, \qquad \chi(\phi) := \sin^{-1}\sqrt{\frac{(\beta_+-\beta_-)\sin^2\phi}{\beta_+(\sin^2\phi-\beta_-)}}. \tag{A.17}$$

$$\int_0^{\phi} d\psi \frac{\ell a \sin^2\psi d\psi}{\sqrt{\cos^2\psi - m^2\sin^2\psi - \ell^2 a^2 \sin^4\psi}} = \frac{1}{2}\int_0^v du \sqrt{\frac{u}{(u-\beta_-)(u-\beta_+)(u-1)}}$$

$$= \frac{(m^2+1)+\sqrt{(m^2+1)^2+4\ell^2a^2}}{2\ell a\left[(m^2+1)^2+4\ell^2a^2\right]^{1/4}}\left[\Pi(\chi(\phi),C,\kappa)-F(\chi(\phi),\kappa)\right]. \tag{A.18}$$

$$\int_0^{\phi} d\psi \frac{m d\psi}{\sqrt{\cos^2\psi - m^2\sin^2\psi - \ell^2 a^2 \sin^4\psi}} = \frac{1}{2\ell a}\int_0^v du \frac{m}{\sqrt{(u-\beta_-)u(u-\beta_+)(u-1)}}$$

$$= m[(m^2+1)^2+4\ell^2a^2]^{-1/4}F(\chi(\phi),\kappa). \tag{A.19}$$

$$\int_{\frac{\epsilon}{R_2}}^{\phi} d\psi \frac{\cot^2\psi d\psi}{\sqrt{\cos^2\psi - m^2\sin^2\psi - \ell^2 a^2 \sin^4\psi}} = \frac{1}{2\ell a}\int_{\frac{\epsilon^2}{R_2^2}}^{v} du \frac{1-u}{u\sqrt{(u-\beta_-)u(u-\beta_+)(u-1)}}$$

$$= \frac{R_2}{\epsilon} + [(m^2+1)^2+4\ell^2a^2]^{1/4}\left[-\cot\chi(\phi)\sqrt{1-\kappa^2\sin^2\chi(\phi)} - E(\chi(\phi),\kappa) + (1-\kappa^2)F(\chi(\phi),\kappa)\right]. \tag{A.20}$$

When $\phi = \phi_0$, each integral becomes a complete elliptic integral, i.e.

$$\int_0^{\phi_0} d\psi \frac{\ell a \sin^2\psi d\psi}{\sqrt{\cos^2\psi - m^2\sin^2\psi - \ell^2 a^2 \sin^4\psi}} = \frac{(m^2+1)+\sqrt{(m^2+1)^2+4\ell^2a^2}}{2\ell a\left[(m^2+1)^2+4\ell^2a^2\right]^{1/4}}\left[\Pi(C,\kappa)-K(\kappa)\right], \tag{A.21}$$

$$\int_0^{\phi_0} d\psi \frac{m d\psi}{\sqrt{\cos^2\psi - m^2\sin^2\psi - \ell^2 a^2 \sin^4\psi}} = m[(m^2+1)^2+4\ell^2a^2]^{-1/4}K(\kappa), \tag{A.22}$$

$$\int_{\frac{\epsilon}{R_2}}^{\phi_0} d\psi \frac{\cot^2\psi d\psi}{\sqrt{\cos^2\psi - m^2\sin^2\psi - \ell^2 a^2 \sin^4\psi}} = \frac{R_2}{\epsilon} + [(m^2+1)^2+4\ell^2a^2]^{1/4}\left[-E(\kappa)+(1-\kappa^2)K(\kappa)\right]. \tag{A.23}$$

B Explicit form of the coulomb coefficient

Here we write the explicit form mentioned in section 4.3.

$$\beta_\pm = \frac{-\gamma \pm \sqrt{\gamma^2+1}}{\ell a}, \qquad \kappa^2 = C = \frac{-\gamma+\sqrt{\gamma^2+1}}{2\sqrt{\gamma^2+1}}, \qquad \sin^2\phi_1 = \frac{-\gamma+\sqrt{\gamma^2+\sin^2\theta_k}}{\ell a},$$

$$\chi(\phi_1) = \sin^{-1}\sqrt{\frac{2(-\gamma+\sqrt{\gamma^2+\sin^2\theta_k})\sqrt{\gamma^2+1}}{(-\gamma+\sqrt{\gamma^2+1})(\sqrt{\gamma^2+\sin^2\theta_k}+\sqrt{\gamma^2+1})}}, \qquad \eta = 1+\frac{1}{2}\left(\frac{L}{R_2}\right)^2. \tag{B.1}$$

B.1 $\theta_k > \pi/2$

γ is related to Θ by

$$\Theta - \theta_k = \frac{\sqrt{\gamma}}{(\gamma^2+1)^{1/4}} F(\chi(\phi_1), \kappa). \tag{B.2}$$

The potential is

$$S_{tot} = 2\pi R_2 \frac{M}{L}, \tag{B.3}$$

where the coefficient can be written as

$$\begin{aligned} M =& \frac{1}{2\pi} \frac{\gamma + \sqrt{\gamma^2+1}}{\sqrt{2}(\gamma^2+1)^{1/4}} \left[\Pi(\chi(\phi_1), \kappa^2, \kappa) - F(\chi(\phi_1), \kappa)\right] \\ & \times \sqrt{\lambda} \Bigg[- \frac{\cos\theta_k}{\sqrt{-\gamma + \sqrt{\gamma^2 + \sin^2\theta_k}}} \\ & + \sqrt{2}(\gamma^2+1)^{1/4} \left\{ - \cot\chi(\phi_1)\sqrt{1-\kappa^2\sin^2\chi(\phi_1)} - E(\chi(\phi_1),\kappa) + (1-\kappa^2)F(\chi(\phi_1),\kappa)\right\} \Bigg]. \end{aligned} \tag{B.4}$$

B.2 $\theta_k < \pi/2$

$$\Theta - \theta_k = \frac{\sqrt{\gamma}}{(\gamma^2+1)^{1/4}} \left[2K(\kappa) - F(\chi(\phi_1), \kappa)\right]. \tag{B.5}$$

$$\begin{aligned} M =& \frac{1}{2\pi} \frac{\gamma + \sqrt{\gamma^2+1}}{\sqrt{2}(\gamma^2+1)^{1/4}} \left[2\Pi(\kappa^2, \kappa) - \Pi(\chi(\phi_1), \kappa^2, \kappa) - 2K(\kappa) + F(\chi(\phi_1), \kappa)\right] \\ & \times \sqrt{\lambda} \Bigg[- \frac{\cos\theta_k}{\sqrt{-\gamma + \sqrt{\gamma^2 + \sin^2\theta_k}}} + \sqrt{2}(\gamma^2+1)^{1/4} \Big\{ \cot\chi(\phi_1)\sqrt{1-\kappa^2\sin^2\chi(\phi_1)} \\ & - 2E(\kappa) + E(\chi(\phi_1),\kappa) + 2(1-\kappa^2)K(\kappa) - (1-\kappa^2)F(\chi(\phi_1),\kappa)\Big\} \Bigg]. \end{aligned} \tag{B.6}$$

References

[1] J. M. Maldacena, *"The large N limit of superconformal field theories and supergravity,"* Adv. Theor. Math. Phys. **2** (1998) 231–252, [hep-th/9711200].

[2] S.-J. Rey and J.-T. Yee, *"Macroscopic strings as heavy quarks in large N gauge theory and anti-de Sitter supergravity,"* Eur. Phys. J. **C22** (2001) 379–394, [hep-th/9803001].

[3] J. M. Maldacena, *"Wilson loops in large N field theories,"* Phys. Rev. Lett. **80** (1998) 4859–4862, [hep-th/9803002].

[4] N. Drukker and B. Fiol, *"All-genus calculation of Wilson loops using D-branes,"* JHEP **02** (2005) 010, [hep-th/0501109].

[5] S. A. Hartnoll and S. Prem Kumar, *"Multiply wound Polyakov loops at strong coupling,"* Phys. Rev. **D74** (2006) 026001, [hep-th/0603190].

[6] S. Yamaguchi, *"Wilson loops of anti-symmetric representation and D5-branes,"* JHEP **05** (2006) 037, [hep-th/0603208].

[7] J. Gomis and F. Passerini, *"Holographic Wilson loops,"* JHEP **08** (2006) 074, [hep-th/0604007].

[8] J. K. Erickson, G. W. Semenoff and K. Zarembo, *"Wilson loops in $N = 4$ supersymmetric Yang-Mills theory,"* Nucl. Phys. **B582** (2000) 155–175, [hep-th/0003055].

[9] N. Drukker and D. J. Gross, *"An exact prediction of $N = 4$ SUSYM theory for string theory,"* J. Math. Phys. **42** (2001) 2896–2914, [hep-th/0010274].

[10] D. Rodriguez-Gomez, *"Computing Wilson lines with dielectric branes,"* Nucl. Phys. **B752** (2006) 316–326, [hep-th/0604031].

[11] K. Okuyama and G. W. Semenoff, *"Wilson loops in $N = 4$ SYM and fermion droplets,"* JHEP **06** (2006) 057, [hep-th/0604209].

[12] S. A. Hartnoll and S. P. Kumar, *"Higher rank Wilson loops from a matrix model,"* JHEP **08** (2006) 026, [hep-th/0605027].

[13] S. A. Hartnoll, *"Two universal results for Wilson loops at strong coupling,"* hep-th/0606178.

[14] B. Chen and W. He, *"On 1/2-BPS Wilson-'t Hooft loops,"* hep-th/0607024.

[15] S. Giombi, R. Ricci and D. Trancanelli, *"Operator product expansion of higher rank Wilson loops from D-branes and matrix models,"* hep-th/0608077.

[16] D. J. Gross and H. Ooguri, *"Aspects of large N gauge theory dynamics as seen by string theory,"* Phys. Rev. **D58** (1998) 106002, [hep-th/9805129].

[17] K. Zarembo, *"Wilson loop correlator in the AdS/CFT correspondence,"* Phys. Lett. **B459** (1999) 527–534, [hep-th/9904149].

[18] P. Olesen and K. Zarembo, *"Phase transition in Wilson loop correlator from AdS/CFT correspondence,"* hep-th/0009210.

[19] H. Kim, D. K. Park, S. Tamarian and H. J. W. Muller-Kirsten, *"Gross-Ooguri phase transition at zero and finite temperature: Two circular Wilson loop case,"* JHEP **03** (2001) 003, [hep-th/0101235].

[20] G. Arutyunov, J. Plefka and M. Staudacher, *"Limiting geometries of two circular Maldacena-Wilson loop operators,"* JHEP **12** (2001) 014, [hep-th/0111290].

[21] A. Tsuji, *"Holography of Wilson loop correlator and spinning strings,"* hep-th/0606030.

[22] C. Ahn, *"Two circular Wilson loops and marginal deformations,"* hep-th/0606073.

[23] K. Zarembo, *"String breaking from ladder diagrams in SYM theory,"* JHEP **03** (2001) 042, [hep-th/0103058].

[24] J. Plefka and M. Staudacher, *"Two loops to two loops in $N = 4$ supersymmetric Yang-Mills theory,"* JHEP **09** (2001) 031, [hep-th/0108182].

[25] S. Yamaguchi, *"Bubbling geometries for half BPS Wilson lines,"* hep-th/0601089.

[26] O. Lunin, *"On gravitational description of Wilson lines,"* JHEP **06** (2006) 026, [hep-th/0604133].

[27] D. Berenstein, R. Corrado, W. Fischler and J. M. Maldacena, *"The operator product expansion for Wilson loops and surfaces in the large N limit,"* Phys. Rev. **D59** (1999) 105023, [hep-th/9809188].

[28] J. Pawelczyk and S.-J. Rey, *"Ramond-Ramond flux stabilization of D-branes,"* Phys. Lett. **B493** (2000) 395–401, [hep-th/0007154].

[29] J. M. Camino, A. Paredes and A. V. Ramallo, *"Stable wrapped branes,"* JHEP **05** (2001) 011, [hep-th/0104082].

[30] N. Drukker, D. J. Gross and H. Ooguri, *"Wilson loops and minimal surfaces,"* Phys. Rev. **D60** (1999) 125006, [hep-th/9904191].

hep-th/0701052

Semi-classical open string corrections and symmetric Wilson loops

Satoshi Yamaguchi
yamaguch@ihes.fr

IHES, Le Bois-Marie, 35, route de Chartres
F-91440 Bures-sur-Yvette, FRANCE

Abstract

In the AdS/CFT correspondence, an $AdS_2 \times S^2$ D3-brane with electric flux in $AdS_5 \times S^5$ spacetime corresponds to a circular Wilson loop in the symmetric representation or a multiply wound one in $N = 4$ super Yang-Mills theory. In order to distinguish the symmetric loop and the multiply wound loop, one should see an exponentially small correction in large 't Hooft coupling. We study semi-classically the disk open string attached to the D3-brane. We obtain the exponent of the term and it agrees with the result of the matrix model calculation of the symmetric Wilson loop.

1 Introduction and summary

Wilson loops are some of the most interesting non-local operators in Yang-Mills theories. In particular the Wilson loops in $N = 4$ super Yang-Mills theory have interesting string theory counterparts in the AdS/CFT correspondence [1]. The Wilson loop in the fundamental representation corresponds to a macroscopic fundamental string in $AdS_5 \times S^5$ spacetime [2, 3]. Moreover the Wilson loops in higher rank representations were recently explored in the AdS/CFT correspondence, the D-brane probe descriptions [2, 4, 5, 6, 7, 8, 9, 10, 11, 12, 13, 14, 15, 16, 17] and the supergravity descriptions [18, 19] were developed.

One of these D-brane probe pictures is the D3-brane description of the symmetric or multiply wound Wilson loop[4]. These two different kind of Wilson loop (the multiply wound Wilson loop and symmetric one) have the same leading term in the expectation value in large λ ('t Hooft coupling) limit. In other words, the difference between these two VEVs is exponentially smaller, like $\exp[-\sqrt{\lambda}(\text{constant})]$, than the expectation values. It was shown in [15] that the D3-brane corresponds to the symmetric Wilson loop from the point of view of the low energy theory on the D-branes. In this letter we want to see this exponentially smaller term in the AdS side of the correspondence.

In order to treat this kind of small correction, one should include some quantum effects in the AdS side of the calculation. In principle, if one sums up all the configurations which satisfy a certain boundary condition at the AdS boundary, one gets the exact result. This set of the configurations includes small massless fluctuation, open strings, D-branes, new geometries and perhaps other things. They may or may not be a solution of the classical equation of motion. The only constraint is the boundary condition at the AdS boundary; the configuration becomes, in the problem here, the single D3-brane with electric flux at the boundary of the AdS. We consider the configuration with a disk open string worldsheet attached to the D3-brane among these configurations since $\exp[-\sqrt{\lambda}(\text{constant})]$ type corrections usually appear as worldsheet non-perturbative[1] corrections.

This kind of worldsheet non-perturbative effects typically appears as worldsheet instantons. In the Wilson loop literature, for example, the open string instanton in the 1/4 BPS Wilson loop captures the exponentially smaller term in the asymptotic expansion of the modified Bessel function [20]. The worldsheet instantons also play a central role in the Wilson loops in the topological large N duality [21].

In this letter, we find that there is also a worldsheet non-perturbative effect in the

[1] Here "worldsheet non-perturbative" means non-perturbative in the worldsheet sense i.e. the correction like $\exp[-(\text{constant})/\alpha']$. It is not non-perturbative in the string theory sense.

open string attached to the D3-brane which corresponds to the symmetric Wilson loop. It captures the exponentially small difference between the symmetric and multiply wound Wilson loops. Actually this difference is calculated using the Gaussian matrix model as eq. (2.19). The open string non-perturbative effect is shown in eq. (3.18). Both of them are written as

$$\exp\left[-\sqrt{\lambda}\left(\sqrt{1+\kappa^2}-1\right)\right], \tag{1.1}$$

where κ is defined as $\kappa := k\sqrt{\lambda}/(4N)$ and k denotes the rank of the symmetric representation. This result support the statement that the D3-brane corresponds to the symmetric Wilson loop, but not the multiply wound Wilson loop.

The construction of this letter is as follows. In section 2 we use the Gaussian matrix model to evaluate the correction in the Yang-Mills theory side. In section 3, we consider the open string on the D3-brane and evaluate the worldsheet non-perturbative correction.

2 Matrix model calculation

In this section, we evaluate the leading difference of the rank k symmetric Wilson loop and k-times wound Wilson loop in $N = 4$ super Yang-Mills theory, by using the Gaussian matrix model[22, 23]. We evaluate it in the following limit.

- First, take $N \to \infty$ with $\lambda := g_{YM}^2 N$ and k/N kept finite.
- Then, take $\lambda \to \infty$ with $\kappa := k\sqrt{\lambda}/(4N)$ kept finite.

This quantity can be calculated in various method (see for example [23, 9, 10] and references therein). Here we put emphasis on the eigenvalue distribution in order to see the pictorial similarity to the AdS side in the next section.

We consider the 1/2 BPS circular Wilson loop $\mathrm{Tr}_R U$ with the representation R of $SU(N)$ and the group element U is defined as

$$U := P\exp\int_C d\tau(\dot{x}^\mu(\tau)iA_\mu(x(\tau)) + |\dot{x}(\tau)|\phi_1(x(\tau))), \tag{2.1}$$

where the trajectory C is a circle, $\dot{x}$ denotes the differential $dx^\mu/d\tau$, A_μ is the gauge field and ϕ_1 is one of the six scalar fields in $N = 4$ super Yang-Mills theory.

Let us introduce some notations in order to express the gauge invariant polynomials. Let $u_1, u_2, \dots, u_N$ be the eigenvalues of the matrix U. Then for the choice of integers $\mu = (\mu_1, \mu_2, \dots, \mu_r)$, $r \le N$, $\mu_1 \ge \mu_2 \ge \dots \ge \mu_r$ the symmetric monomial $m_\mu(U)$ is defined as

$$m_\mu(U) = u_1^{\mu_1}u_2^{\mu_2}\dots u_r^{\mu_r} + (\text{symmetrization}). \tag{2.2}$$

The k-times wound Wilson loop is expressed by these notations as $\operatorname{tr} U^k = m_{(k)}(U) = \sum_{i=1}^N u_i^k$. On the other hand, the rank k symmetric Wilson loop $\operatorname{Tr}_{S_k} U$ is the sum of all the monomials of degree k as

$$\operatorname*{Tr}_{S_k} U = \sum_{\mu:\ k \text{ boxes}} m_\mu(U) = m_{(k)}(U) + m_{(k-1,1)}(U) + \cdots . \tag{2.3}$$

Therefore in order to distinguish $\operatorname{Tr}_{S_k} U$ and $m_{(k)}(U)$ we should see $\langle m_{(k-1,1)}(U)\rangle / \langle m_{(k)}(U)\rangle$. This is what we want to evaluate here.

It is conjectured[22, 23] that the expectation value of this Wilson loop is calculated by the Gaussian matrix model. Let Y be an $N \times N$ Hermitian matrix and "tr" be the trace in fundamental representation. The expectation value is calculated as

$$\langle m_\mu(U)\rangle = \left\langle m_\mu(e^Y)\right\rangle_{mm} := \frac{1}{Z}\int dY\ m_\mu(e^Y) \exp\left(-\frac{2N}{\lambda}\operatorname{tr}[Y^2]\right), \tag{2.4}$$

$$Z := \int dY \exp\left(-\frac{2N}{\lambda}\operatorname{tr}[Y^2]\right). \tag{2.5}$$

The standard method to evaluate this integral is to diagonalize the matrix Y. The matrix integral above is rewritten in terms of the eigenvalues

$$\left\langle m_\mu(e^Y)\right\rangle_{mm} = \frac{1}{Z}\int \prod_{i=1}^N dy_i\ m_\mu(e^y) \exp\left(-I[y]\right), \tag{2.6}$$

$$Z := \int \prod_{i=1}^N dy_i \exp\left(-I[y]\right), \tag{2.7}$$

$$I[y] := \frac{2N}{\lambda}\sum_{i=1}^N y_i^2 - 2\sum_{i<j}\log|y_i - y_j|. \tag{2.8}$$

Let us review some fact in the large N limit of the Gaussian matrix model. In the large N limit, the eigenvalue distribution follows Wigner's semi-circle law

$$\left\langle \sum_{i=1}^N \delta(z - y_i)\right\rangle_{mm} = \begin{cases} \frac{2N}{\pi\lambda}\sqrt{\lambda - z^2} & (-\sqrt{\lambda} \le z \le \sqrt{\lambda}) \\ 0 & (z \le -\sqrt{\lambda} \text{ or } z \ge \sqrt{\lambda}) \end{cases}. \tag{2.9}$$

The resolvent is also useful

$$w(z) := \left\langle \sum_{i=1}^N \frac{1}{y_i - z}\right\rangle_{mm} = \frac{2N}{\lambda}\left(-z + \sqrt{z^2 - \lambda}\right). \tag{2.10}$$

First we evaluate the k-times wound loop $\left\langle m_{(k)}(e^Y)\right\rangle_{mm}$.

$$\left\langle m_{(k)}(e^Y)\right\rangle_{mm} = \frac{N}{Z}\int \prod_{i=1}^N dy_i \exp\left(-I[y] + k y_1\right). \tag{2.11}$$

We evaluate (2.11) by the saddle point. The equations of motion for $y_2 \dots y_N$ are the same as $k = 0$ case. On the other hand, the equation of motion for y_1 becomes

$$0 = \frac{\partial}{\partial y_1}(I[y] - ky_1) = \frac{4N}{\lambda}y_1 - 2\sum_{j=2}^{N}\frac{1}{y_1 - y_j} - k. \tag{2.12}$$

Actually the back-reaction of y_1 on $y_2, \dots, y_N$ is negligible in the large λ limit. Thus we solve eq. (2.12) in the semi-circle distribution for $y_2, \dots, y_N$. The second term in eq.(2.12) can be expressed by the resolvent of (2.10). Then eq.(2.12) is solved as

$$y_1 = \sqrt{\lambda}\sqrt{1+\kappa^2}, \qquad \kappa = \frac{k\sqrt{\lambda}}{4N}. \tag{2.13}$$

Let us define $\mathcal{F}_{(k)}$ by

$$\left\langle m_{(k)}(e^Y)\right\rangle_{mm} =: \exp(-\mathcal{F}_{(k)}). \tag{2.14}$$

We can approximate the integral (2.11) as

$$\begin{aligned}\mathcal{F}_{(k)} &= (\text{constant}) + (I[y] - ky_1)\big|_{y_1=\sqrt{\lambda}\sqrt{1+\kappa^2}} \\ &= -2N(\kappa\sqrt{1+\kappa^2} + \sinh^{-1}\kappa).\end{aligned} \tag{2.15}$$

The (constant) in the above equation is determined so that $\mathcal{F}_{(0)} = 0$. This is the same result as in [4].

Next, we turn to the calculation of $\left\langle m_{(k-1,1)}(e^y)\right\rangle_{mm}$. This expectation value is written as

$$\left\langle m_{(k-1,1)}(e^Y)\right\rangle_{mm} = \frac{N(N-1)}{Z}\int\prod_{i=1}^{N}dy_i \exp\left(-I[y] + (k-1)y_1 + y_2\right). \tag{2.16}$$

Since y_1 and y_2 are distant enough in the large λ limit, we can ignore the interaction between them. Therefore the solutions of the equations of motion becomes

$$y_1 = \sqrt{\lambda}\sqrt{1+\left(\frac{(k-1)\sqrt{\lambda}}{4N}\right)^2}, \qquad y_2 = \sqrt{\lambda}. \tag{2.17}$$

This eigenvalue distribution looks like figure 1. We evaluate the integral (2.16) by using the solution (2.17) and obtain

$$\left\langle m_{(k-1,1)}(e^Y)\right\rangle_{mm} = \exp\left[-\mathcal{F}_{(k-1)} + \sqrt{\lambda}\right] = \exp\left[-\mathcal{F}_{(k)} - \sqrt{\lambda}\sqrt{1+\kappa^2} + \sqrt{\lambda}\right]. \tag{2.18}$$

The final result of this section is

$$\frac{\left\langle m_{(k-1,1)}(U)\right\rangle}{\left\langle m_{(k)}(U)\right\rangle} = \frac{\left\langle m_{(k-1,1)}(e^Y)\right\rangle_{mm}}{\left\langle m_{(k)}(e^Y)\right\rangle_{mm}} = \exp\left[-\sqrt{\lambda}(\sqrt{1+\kappa^2} - 1)\right]. \tag{2.19}$$

This is actually exponentially small in the large λ limit. In the next section, we will compare this exponent to the worldsheet non-perturbative correction.

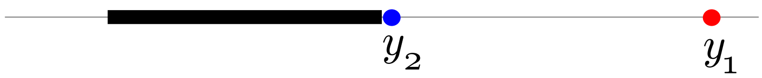

Figure 1: The eigenvalue distribution which dominates the expectation value $\langle m_{(k-1,1)}(e^Y)\rangle_{mm}$. The black thick line denotes the semi-circle distribution of eigenvalues $y_3, \ldots, y_N$.

3 Disk worldsheet corrections

In this section, we will consider the disk open string whose boundary is attached to the $AdS_2 \times S^2$ D3-brane, and compute the disk open string amplitudes by using the semi-classical technique. We concentrate on the exponent of the correction in the large λ limit. We postpone the integral on the moduli space and the one-loop determinant to future works. We find that the exponent of the correction agree with the matrix model result (2.19).

Actually, there are perturbative corrections to the expression (2.15). We might not be allowed to retain the non-perturbative correction calculated in this section, since it is much smaller than the perturbative corrections. This may be justified by the supersymmetry but we leave it to future works.

It is convenient to use the coordinate system of [4]. The metric of AdS_5 is expressed as

$$ds^2 = \frac{L^2}{\sin^2\eta}\left[d\eta^2 + \cos^2\eta d\psi^2 + d\rho^2 + \sinh^2\rho(d\theta^2 + \sin^2\theta d\phi)\right], \qquad L^2 = \alpha'\sqrt{\lambda},$$
$$0 \leq \eta \leq \frac{\pi}{2}, \qquad 0 \leq \psi \leq 2\pi, \qquad 0 \leq \rho, \qquad 0 \leq \theta \leq \pi, \qquad 0 \leq \phi \leq 2\pi. \tag{3.1}$$

The $AdS_2 \times S^2$ D3-brane worldvolume [2, 4] is expressed in this coordinate system as

$$\sinh\rho = \kappa\sin\eta, \qquad \kappa = \frac{k\sqrt{\lambda}}{4N}. \tag{3.2}$$

The electric field on the D3-brane worldvolume is excited and takes the value

$$F = dA = i\frac{\sqrt{\lambda}}{2\pi}\frac{\kappa}{\sinh^2\rho}d\psi d\rho, \tag{3.3}$$

where we identify ψ and ρ as worldvolume coordinates.

Now let us consider the disk string worldsheet whose boundary is attached to the D3-brane expressed by eqs.(3.2),(3.3). Let the worldsheet coordinates be (σ, χ). The coordinate σ, $(\sigma_0 \leq \sigma \leq \sigma_1)$ is the radial coordinate of the disk. $\sigma = \sigma_0$ corresponds to the boundary, while $\sigma = \sigma_1$ to the center of the disk. The other coordinate χ, $(0 \le \chi \le 2\pi)$ is the angular coordinate of the disk. The string worldsheet action is written as

$$S = S_{bulk} + S_{bdy}, \qquad S_{bulk} = \frac{1}{2\pi\alpha'} \int d\sigma d\chi \sqrt{\det G}, \qquad S_{bdy} = i \int_{\sigma=\sigma_0} A, \tag{3.4}$$

where G is the induced metric and A is the gauge field (3.3).

In this letter, we consider the following special ansatz.

$$\eta = \eta(\sigma), \qquad \rho = \rho(\sigma), \qquad \psi = \chi, \qquad \theta = 0. \tag{3.5}$$

Since the center of the worldsheet $\sigma = \sigma_1$ is one point and should be mapped to one point in spacetime, the condition $\eta(\sigma_1) = \pi/2$ is imposed. Meanwhile the boundary value of η is denoted by $\eta(\sigma_0) = \eta_0$. This boundary of the string is attached to the D3-brane (3.2), and it gives a constraint on the boundary value of ρ as $\rho(\sigma_0) = \sinh^{-1}(\kappa \sin \eta_0)$.

Putting this ansatz into the action (3.4), we obtain (prime " $'$ " denotes the σ derivative)

$$S_{bulk} = \sqrt{\lambda} \int_{\sigma_0}^{\sigma_1} d\sigma \frac{\cos\eta}{\sin^2\eta} \sqrt{\eta'^2 + \rho'^2}, \tag{3.6}$$

$$S_{bdy} = \sqrt{\lambda} \left(\sqrt{1+\kappa^2} - \frac{\sqrt{1+\kappa^2 \sin^2\eta_0}}{\sin\eta_0} \right). \tag{3.7}$$

The constant shift of the boundary action (3.7) is fixed so that $S_{bdy} = 0$ at $\eta_0 = \pi/2$ where the boundary of the worldsheet shrinks to a point.

If we fix the boundary value η_0, the bulk action (3.6) has the lower bound

$$S_{bulk} \ge \sqrt{\lambda} \int_{\sigma_0}^{\sigma_1} d\sigma \frac{\cos\eta}{\sin^2\eta} \eta' = \sqrt{\lambda} \left(-1 + \frac{1}{\sin\eta_0} \right). \tag{3.8}$$

This bound (3.8) is saturated when

$$\rho' = 0 \qquad \Rightarrow \qquad \rho = (\text{constant}) = \sinh^{-1}(\kappa \sin\eta_0). \tag{3.9}$$

This configuration (3.9) actually satisfies the equations of motion derived from the bulk action (3.6). This configuration is shown in figure 2.

When we derive the bound (3.8), we assume the boundary $\eta(\sigma_0) = \eta_0$ is fixed. However this is not the true boundary condition; the boundary of the string worldsheet can move along the D3-brane. In this sense the configuration (3.9) is not a stationary point of the action.

Though the configuration (3.9) is not a solution, it is still useful to evaluate the path-integral; it is "the bottom of the trough" [24]. We explain here how to evaluate the

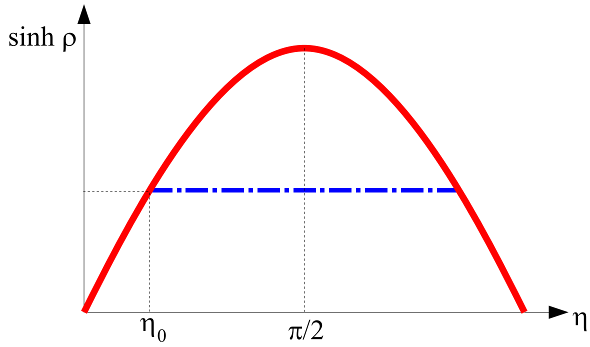

Figure 2: The configuration (3.9) is shown in the ρ-η plane. The red solid line expresses the D3-brane (3.2), while the blue dash-dotted line expresses the open string (3.9) ending on the D3-brane at $\eta = \eta_0$.

path-integral using the configuration (3.9). We want to evaluate the path-integral

$$J = \int D\eta D\rho \;\exp\left(-S\right), \tag{3.10}$$

with the correct boundary condition determined by the configuration of the D3-brane. This integral can be rewritten as

$$J = \int d\eta_0 \widetilde{J}(\eta_0), \qquad \widetilde{J}(\eta_0) = \int_{\eta(\sigma_0)=\eta_0} D\eta D\rho \;\exp\left(-S\right). \tag{3.11}$$

In the path-integral $\widetilde{J}(\eta_0)$ the boundary value of η is fixed to η_0. Hence (3.9) is the saddle point of this integral. The path-integral $\widetilde{J}(\eta_0)$ can be evaluated by the point.

$$\widetilde{J}(\eta_0) = \exp\left(-\widetilde{S}(\eta_0)\right), \tag{3.12}$$

$$\widetilde{S}(\eta_0) = (S_{bulk} + S_{bdy})|_{\rho=\sinh^{-1}(\kappa\sin\eta_0)} = \sqrt{\lambda}\left(\sqrt{1+\kappa^2} - 1 + \frac{1-\sqrt{1+\kappa^2\sin^2\eta_0}}{\sin\eta_0}\right). \tag{3.13}$$

The η_0 integral in (3.11) is written as

$$J = \int_0^{\pi/2} d\eta_0 \exp[-\widetilde{S}(\eta_0)] = \exp[-T(\pi/2)] - \exp[-T(0)], \tag{3.14}$$

where $T(\eta_0)$ is defined as a solution of

$$T(\eta_0) - \log\frac{dT}{d\eta_0}(\eta_0) = \widetilde{S}(\eta_0). \tag{3.15}$$

Since $\widetilde{S}(\eta_0)$ is proportional to $\sqrt{\lambda}$, we can take $T(\eta_0)$ as

$$T(\eta_0) = \widetilde{S}(\eta_0) + O(\log\sqrt{\lambda}). \tag{3.16}$$

The first term on the right-hand side of eq.(3.14) is

$$\exp[-T(\pi/2)] = \exp[-\widetilde{S}(\pi/2) + O(\log\sqrt{\lambda})] = (\text{powers of } \lambda). \tag{3.17}$$

Thus this term captures the perturbative corrections. The second term on the right-hand side of eq.(3.14) is the exponentially small term that we want to see here. It is written as

$$\exp[-T(0)] = \exp\left[-\widetilde{S}(0) + O(\log\sqrt{\lambda})\right] \cong \exp\left[-\sqrt{\lambda}\left(\sqrt{1+\kappa^2}-1\right)\right]. \tag{3.18}$$

This is the main result of this letter. The result (3.18) agrees with the matrix model result (2.19).

This small non-perturbative effect can be understood qualitatively as follows. There are two forces acting on the string end point: the string tension pulling the end point inside, and the electric force pushing the end point outside. The string tension is always larger than the electric force, and there is no stationary point other than the constant map. However, as the string worldsheet becomes larger and larger, the difference of these two forces becomes smaller and smaller. Actually when the worldsheet is large enough ($\eta_0 \ll 1$), the two forces almost cancel each other and the worldsheet boundary can be moved almost freely without increasing or decreasing the action. In other words, however large the worldsheet becomes, the action remains finite. The correction (3.18) is the result of this effect.

This kind of exotic effect is not present for a flat D-brane in the flat space. In this case, the action diverges as the worldsheet becomes larger. Thus the contribution to the amplitudes is zero. Therefore the DBI action does not capture this effect since it is based on the small curvature approximation.

There is an intuitive explanation why the configuration (3.9) with $\eta_0 \sim 0$ produces the term $\left\langle m_{(k-1,1)}(e^Y)\right\rangle_{mm}$. It is proposed in [18][2] how the eigenvalue distribution of the Gaussian matrix model can be seen in $AdS_5 \times S^5$. Figure 3 represents the configuration (3.9) in the picture of [18]. When η_0 is close enough to 0, this picture around center is similar to figure 1; the fundamental string looks like y_2 and the D3-brane look like y_1 around the center[3].

[2]Taking the result of this letter into account, the black and white pattern in supergravity solution in [18] interpreted as the eigenvalue distribution of the leading monomial of the representation expressed by a Young diagram. We can guess that there are corrections from the large closed strings, D-branes, geometry and so on. This is also an interesting future problem.

[3]This fundamental string, even when $\eta_0 \to 0$, is supposed to be different from the one used in the circular fundamental Wilson loop [25]. One can distinguish these two, for example, by the value of the action. Our string attached to the D3-brane has the action $\lim_{\eta_0\to 0}\widetilde{S}(\eta_0) = \sqrt{\lambda}\left(\sqrt{1+\kappa^2}-1\right)$. On the other hand the on-shell action of the string which represent the fundamental Wilson loop is $(-\sqrt{\lambda})$.

From the similar point of view, one may guess a branched D3-brane configuration, shown in figure 4, contributes as another monomial in the symmetric Wilson loop. Calculating this contribution is an interesting future problem.

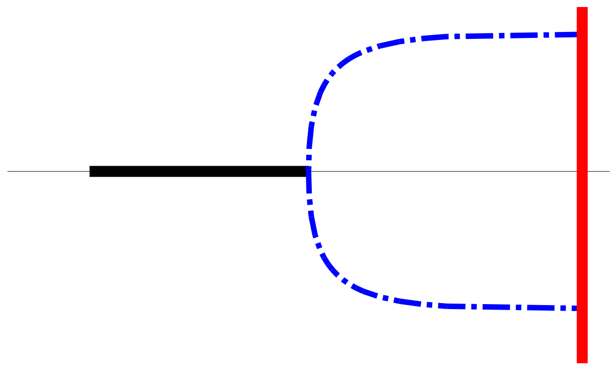

Figure 3: The configuration (3.9) in the picture of [18]. The horizontal direction is "x" of [18], while vertical direction is the radial direction of AdS_2 fiber. The D3-brane is represented by the red solid vertical line. The fundamental string is represented by the blue dash-dotted line.

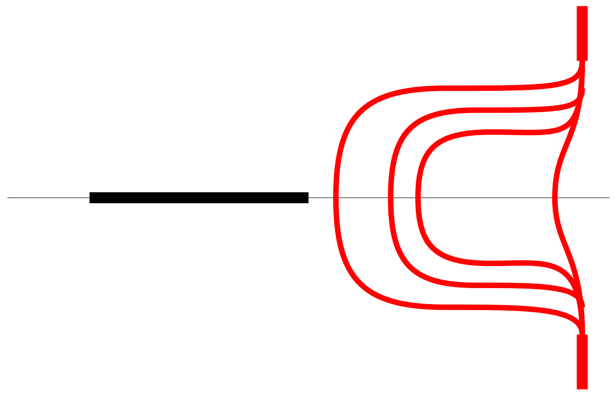

Figure 4: The branched D3-brane configuration expected to correspond to a monomial in the symmetric representation.

Acknowledgment

I would like to thank Gordon W. Semenoff for useful discussions. I am also grateful to Nadav Drukker for careful reading of the manuscript and useful comments. This work was supported in part by the European Research Training Network contract 005104 "ForcesUniverse."

References

[1] J. M. Maldacena, "The large N limit of superconformal field theories and supergravity," Adv. Theor. Math. Phys. **2** (1998) 231–252 [arXiv:hep-th/9711200].

[2] S.-J. Rey and J.-T. Yee, "Macroscopic strings as heavy quarks in large N gauge theory and anti-de Sitter supergravity," Eur. Phys. J. **C22** (2001) 379–394 [arXiv:hep-th/9803001].

[3] J. M. Maldacena, "Wilson loops in large N field theories," Phys. Rev. Lett. **80** (1998) 4859–4862 [arXiv:hep-th/9803002].

[4] N. Drukker and B. Fiol, "All-genus calculation of Wilson loops using D-branes," JHEP **02** (2005) 010 [arXiv:hep-th/0501109].

[5] S. A. Hartnoll and S. Prem Kumar, "Multiply wound Polyakov loops at strong coupling," Phys. Rev. **D74** (2006) 026001 [arXiv:hep-th/0603190].

[6] S. Yamaguchi, "Wilson loops of anti-symmetric representation and D5-branes," JHEP **05** (2006) 037 [arXiv:hep-th/0603208].

[7] J. Gomis and F. Passerini, "Holographic Wilson loops," JHEP **08** (2006) 074 [arXiv:hep-th/0604007].

[8] D. Rodriguez-Gomez, "Computing Wilson lines with dielectric branes," Nucl. Phys. **B752** (2006) 316–326 [arXiv:hep-th/0604031].

[9] K. Okuyama and G. W. Semenoff, "Wilson loops in N = 4 SYM and fermion droplets," JHEP **06** (2006) 057 [arXiv:hep-th/0604209].

[10] S. A. Hartnoll and S. Prem Kumar, "Higher rank Wilson loops from a matrix model," JHEP **08** (2006) 026 [arXiv:hep-th/0605027].

[11] S. A. Hartnoll, "Two universal results for Wilson loops at strong coupling," arXiv:hep-th/0606178.

[12] B. Chen and W. He, "On 1/2-BPS Wilson-'t Hooft loops," arXiv:hep-th/0607024.

[13] S. Giombi, R. Ricci, and D. Trancanelli, "Operator product expansion of higher rank Wilson loops from D-branes and matrix models," arXiv:hep-th/0608077.

[14] T.-S. Tai and S. Yamaguchi, "Correlator of fundamental and anti-symmetric Wilson loops in AdS/CFT correspondence," arXiv:hep-th/0610275.

[15] J. Gomis and F. Passerini, "Wilson loops as D3-branes," arXiv:hep-th/0612022.

[16] N. Drukker, S. Giombi, R. Ricci, and D. Trancanelli, "On the D3-brane description of some 1/4 BPS Wilson loops," arXiv:hep-th/0612168.

[17] T.-S. Tai, "Two Polyakov loop correlators from D5-branes at finite temperature," arXiv:hep-th/0701006.

[18] S. Yamaguchi, "Bubbling Geometries for Half BPS Wilson Lines," arXiv:hep-th/0601089.

[19] O. Lunin, "On gravitational description of Wilson lines," JHEP **06** (2006) 026 [arXiv:hep-th/0604133].

[20] N. Drukker, "1/4 BPS circular loops, unstable world-sheet instantons and the matrix model," JHEP **09** (2006) 004 [arXiv:hep-th/0605151].

[21] J. Gomis and T. Okuda, "Wilson loops, geometric transitions and bubbling Calabi-Yau's," arXiv:hep-th/0612190.

[22] J. K. Erickson, G. W. Semenoff, and K. Zarembo, "Wilson loops in N = 4 supersymmetric Yang-Mills theory," Nucl. Phys. **B582** (2000) 155–175 [arXiv:hep-th/0003055].

[23] N. Drukker and D. J. Gross, "An exact prediction of N = 4 SUSYM theory for string theory," J. Math. Phys. **42** (2001) 2896–2914 [arXiv:hep-th/0010274].

[24] S. R. Coleman, "The uses of instantons." Lecture delivered at 1977 Int. School of Subnuclear Physics, Erice, Italy, Jul 23-Aug 10, 1977.

[25] D. Berenstein, R. Corrado, W. Fischler, and J. M. Maldacena, "The operator product expansion for Wilson loops and surfaces in the large N limit," Phys. Rev. **D59** (1999) 105023 [arXiv:hep-th/9809188].